Journal of Materials Chemistry B

Accepted Manuscript

ROYAL SOCIETY OF CHEMISTRY

www.rsc.org/materialsB

Journal of Materials Chemistry B

REVIEW ARTICLE

Recent Advances in Gold Nanoparticle-Based Bioengineering Applications

Received 00th January 20xx,
Accepted 00th January 20xx

DOI: 10.1039/x0xx00000x

www.rsc.org/

Eun Young Kim,[a] Dinesh Kumar,[b] Gilson Khang[a] and Dong-Kwon Lim*[,b]

Plasmonic nanoparticle based nanotechnology plays a pivotal role in the recent advances in biomedical applications. Along with biocompatibility and robust surface chemistry, the tunable optical properties of the visible and near-infrared regions of gold nanoparticles have attracted significant attention for a wide range of biomedical applications such as *in-vitro* biosensing, *in-vivo* imaging, drug delivery, and tissue engineering. In this review we focus on the the recent advances in biomedical applications based on the use of plasmonic nanoparticles, which have been developed to solve the limitations of current technologies in biosensing, bioimaging, therapeutic drug delivery, and tissue engineering applications.

1. Introduction

The bulk state of the gold alloy has been used to treat oral cavities since the 16th century,[1] and the salt form of gold (I) (i.e., gold sodium thiomalate) has been used to treat a wide variety of rheumatic diseases such as psoriatic arthritis,[2] juvenile arthritis, and discoid lupus erythematous. However, after 1935, its use has been largely superseded by newer drugs.[3, 4] Currently, gold is experiencing another golden age for new technological innovations.[5] Small clusters of gold (0) in the nanoscale range opened a new avenue of applications because of the useful physical and chemical properties of gold nanoparticles (AuNPs). AuNPs demonstrate strong light absorption and scattering properties in the visible and near-infrared (NIR) regions because of surface plasmon resonance (SPR), which can be defined as collective oscillation of conductive electrons.[6, 7] Scientists in the field of nanotechnology have investigated methods of exploiting the unique optical properties of AuNPs to generate various breakthrough technologies in the fields of bioscience, biomedical engineering, and material science for energy applications.[8, 9] Some of these technologies have been successfully commercialized as new tools for clinical diagnosis (Verigene® system by Nanosphere) and drug discovery (Biacore® SPR system by GE).

Along with their unique optical properties, the biocompatibility, simple method for synthesis, robust surface chemistry, and colloidal stability of AuNPs led to the widespread use of AuNPs for biosensing applications. Paper-based devices, called lateral flow biosensors, will be another good example of the use of AuNPs as a sensitive and stable labeling material for biosensors that can be detected by the naked eye.[10] In contrast, silver nanoparticles (AgNPs) have also been used as a class of broad-spectrum antimicrobial reagents in medical and consumer products such as household antiseptic sprays and antimicrobial coating for medical devices. Due to their low colloidal stability and cytotoxicity,[11] AgNPs were not as popular as AuNPs in biomedical engineering.

The optical properties of AuNPs are easily tunable, and the individual nanoparticle structures can be changed to create new structures such as gold nanospheres (AuNPs),[12] nanorods (AuNRs),[13] nanoshells (AuNSs),[14] nanostars (AuSTs),[15] and nanocages (AuCGs)[13, 16] because of the unique SPR modes of each unique structure. Forming assemblies with nanoparticles is another way of controlling the optical properties of AuNPs by changing the coupled state of localized SPR (LSPR), which depends on the assembled structure and the particle distance in assembly.[17-21] For example, a sensitive optical property change based on the particle distance was first applied in a simple colorimetric DNA detection scheme in solution. This technique was simple and sensitive enough to detect single base mismatch between oligonucleotide sequences.[22] The sensitive change in scattering properties between particles, called a plasmon ruler,[23, 24] was also applied to overcome the intrinsic limitations of the förster radius (< 100 Å) of conventional fluorescence resonance energy transfer (FRET)-based methods. Furthermore, the distance dependent quenching properties of fluorescence molecules at close proximity to AuNPs was applied to detect target nucleic acids with high sensitivity and multiplexing capability (called molecular beacon (MB)).[25]

The interactions between light and AuNPs could be further manipulated to generate innovative biomedical engineering technologies with the help of recent advances in nanobio plasmonics for theory, synthesis, and applications as investigated in the past 20 years. In this review, we focus on

[a] Department of BIN Fusion Technology, Department of PolymerNano science & Polymer BIN Research Center, Chonbuk National University, 567 Baekje-daero, Deokjin-gu, Jeonju 561-756, Republic of Korea.
[b] KU-KIST Graduate School of Converging Science and Technology, Korea University, 145 Anam-ro, Seongbuk-gu, Seoul 136-701, Republic of Korea.
E-mail: dklim@korea.ac.kr

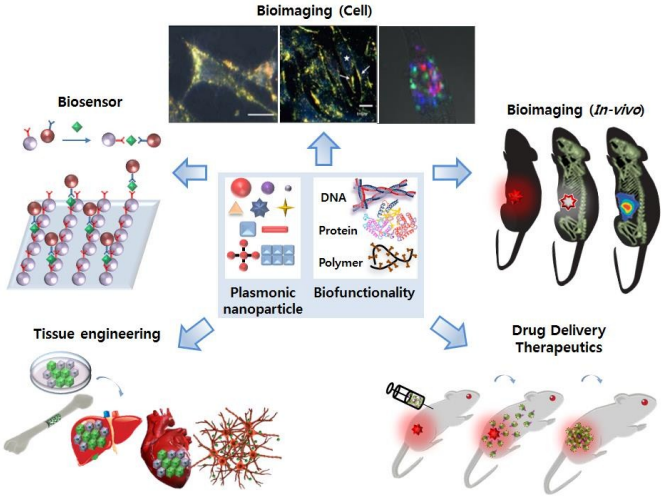

Fig. 1 Developments in plasmonic nanoparticle-based biomedical engineering, such as biosensors, *in vitro* and *in vivo* bioimaging, drug delivery systems, and tissue engineering.

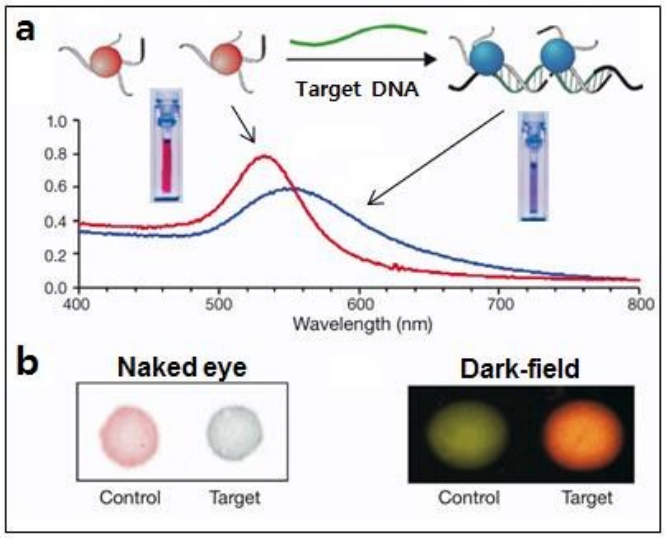

Fig. 2 (a) LSPR changes depend on particle distance with binding target DNA, solution color, and extinction spectra changes. (b) Spot and read with the naked eye and dark-field. (Reprinted with permission from ref. [27] Copyright 2004, Nature publishing group).

current state-of-the-art developments and challenges in AuNP-based applications such as in biosensing and bioimaging for sensitive disease diagnostics, drug delivery for improved therapeutics, and tissue engineering for future innovative biotechnology (Fig. 1). We have discussed representative AuNP-based biosensing schemes and highlighted their individual working principles to detect target substances. We also provide a detailed review on the recent advances in new technologies for cell imaging, *in-vivo* imaging technologies, drug delivery systems, and tissue engineering. In conclusion, we offer a perspective for future biomedical engineering based on the AuNPs discussed.

2. Biosensing applications

Gold nanoparticles have been applied to a variety of biosensing schemes and signal amplification strategies based on unique optical, chemical, and physical properties. Two different categories of biosensing schemes and developed methods for signal amplification are mainly discussed.

2.1 Localized Surface Plasmon Resonance (LSPR) Sensing

Sensitive and reliable diagnostic tools are required for early detection of many fatal diseases. The two key *in-vitro* clinical diagnostic tools widely used are dependent on enzymatic amplification steps and optical signal-based detection methods such as polymerase chain reaction (PCR) for DNA targets or enzyme-linked immunosorbent assay (ELISA) for protein target and fluorescence or chemiluminescence signals.[26] These methods intrinsically require multiple steps and trained expertise to obtain reproducible results and show limited multiplexing capability, which is strongly required for high-throughput assays. In this regard, the use of plasmonic nanoparticles can provide new opportunities to generate cost-effective, point-of-care biosensors with high sensitivity and multiplexing capability. There are two different types of SPR sensors, namely propagating SPR (PSPR) sensors and LSPR sensors. PSPR is usually excited on continuous thin metal films through prism couplers or grating, and PSP resonance can propagate along the metal/dielectric surface up to hundreds of micrometers. However, LSPR is a nonpropagating surface plasmon excited on nanostructured metal surfaces, and LSP resonance can be tuned by their size, shape, and nanoparticle composition.[28,29] The first colorimetric assay for oligonucleotide detection using gold nanoparticle reported by Mirkin *et al*. is a good example of LSPR based sensing.[20] Aggregation of DNA-modified AuNPs in the presence of target DNA in solution, through sequence specific DNA hybridization, leads to a significant decrease in particle distances. This induce subsequent LSPR changes and the solution color change from red wine to blue with dampening of the UV-visible spectra as shown in Fig. 2a. The relatively low sensitivity (nM range) of simple colorimetric assays was greatly improved by incorporating waveguide light scattering, as shown by Storhoff *et al*. (Fig. 2b).[27] The simple "spot and read" colorimetric detection method to identify nucleic acid sequences demonstrated zeptomolar sensitivity with a color change that is visually detectable when the solutions are spotted onto a white-light illuminated glass waveguide (Fig. 2b).[27]

In the case of protein target detection, the aggregation in solution based colorimetric assay showed limited sensitivity because of the relatively large size of protein targets. These induced very little change in the LSPR spectra because of the long distance between AuNPs, even in the aggregated state.[30] For protein target detection, more sophisticated and rationally designed detection scheme is required. The LSPR position of single nanoparticles is also highly sensitive to any changes in the refractive index of the immediate environment of the nanoparticle.[28] Subtle changes in the LSPR of single nanoparticles could be further enhanced by using hot-spot position controlled AuNR structures as LSPR substrates (Fig. 3(a-c)).[31] The highly localized SPR at the end of AuNR, and the binding of protein at this site could significantly increase LSPR changes.[31] The LSPR change could be further

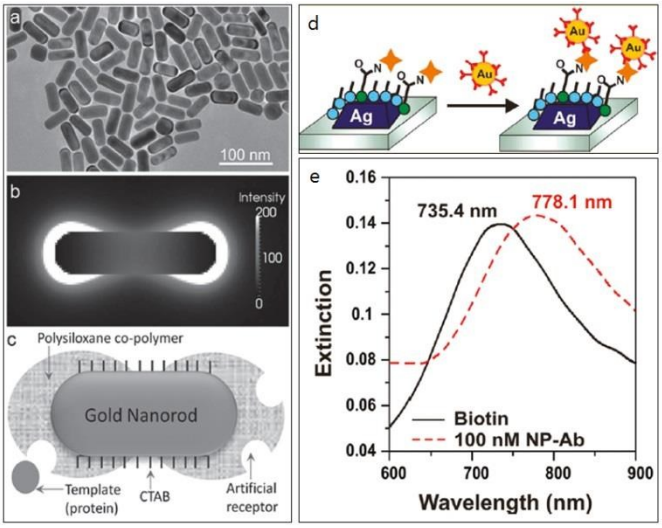

Fig. 3 (a) TEM images of AuNRs. (b) Electromagnetic field distributions of AuNR. (c) Highly localized surface plasmon resonance at the end of AuNRs. (d, e) The use of antibody conjugated AuNPs to enhance LSPR changes. (Reprinted with permission from ref. [29, 31] Copyright 2011, American Chemical Society, Copyright 2013, Wiley).

enhanced by incorporating additional antibody conjugated AuNP probes (Fig. 3d).[29] The use of additional antibody conjugated AuNP probes could induce greater changes in the local environment around the nanoparticle, leading to improvement of the limit of detection by nearly 3 orders of magnitude (Fig. 3e).[29]

2.2 Propagating Surface Plasmon Resonance (PSPR) Sensing

PSPR is usually excited on continuous metal thin films through prism couplers or grating. Although LSPR sensors have much better spectral tunability, their sensitivities are orders of magnitude lower than those of PSPR sensors.[32] PSPR based sensing is more suitable for high-throughput assay systems to study the interactions between biomolecules of interest in real-time. A wide variety of biomolecule targets have been investigated such as DNA, antibody, pathogen, ions (i.e., Mg^{2+}, Ca^{2+}), and drugs with a sensitivity ranging from pM to fM.[32] The signal intensity of PSPR could also be greatly improved by incorporating AuNPs, based on the same signal amplification strategies used in LSPR-based biosensing (Fig. 3(d, e)).

Recently reported unique strategies also showed promising results. Kocabas *et al*. proposed the use of graphene coated Au film to improve SPR sensitivity.[33] They demonstrated an increase in SPR sensitivity with increasing number of graphene layers. This enhancement effect was mainly due to a charge transfer from the surface of graphene to the surface of the Au thin film (Fig. 4(a, b)). The charge transfer led to a stronger excited electric field on the surface of the Au thin film and made the sensing surface more sensitive towards the change in its surrounding medium.[33] The geometry of Au film also greatly influenced the sensitivity of PSPR based sensing. Lee *et al*. reported the use of nanohole arrays instead of flat gold film to improve the current sensitivity of PSPR (Fig. 4c).[34] In this study, the target was exosomes, which are potential disease biomarkers that contain

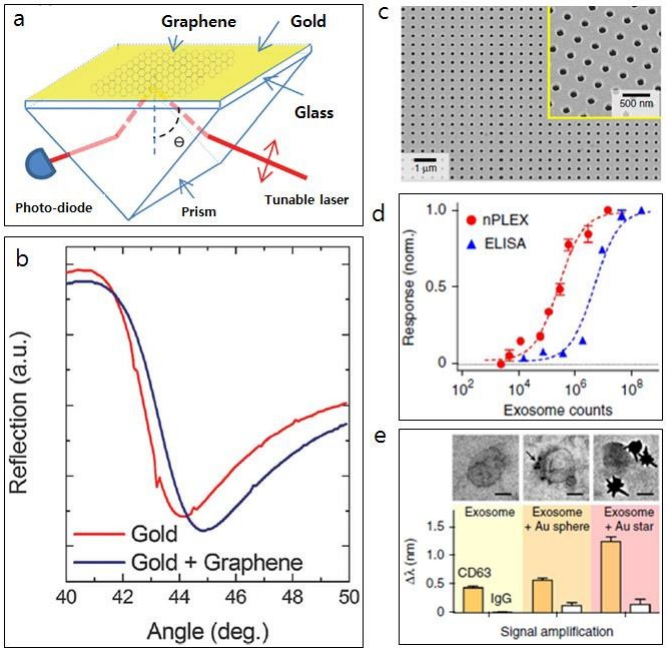

Fig. 4 (a) The SPR sensor with graphene coated Au film. (b) Angle changes before and after graphene coating. (c) The nanohole array Au film. (d) Assay results with ELISA and nanohole SPR sensor (nPLEX). (e) Signal amplification with gold nanoparticle. (Reprinted with permission from ref. [33,34] Copyright 2012, AIP Publishing, Copyright 2014, Nature publishing group).

molecular information about the cells of interest. The sensitivity for exosome detection was 2 orders of magnitude higher than that of conventional ELISA (Fig. 4d). Additional improvement of the sensitivity was possible using AuNPs as shown in Fig. 4e.[34]

2.3 Signal Amplifications

Use of near field enhancement of the electromagnetic field on plasmonic surfaces or the junction between particles significantly improved surface-enhanced Raman scattering (SERS) signals, which could be applied to detect multiple targets with femto-molar sensitivity.[35] The single molecule sensitivity of SERS has already been proven, but its practical use as a robust sensing method to obtain quantitative responses with signal reproducibility is of paramount importance, and needs to be properly addressed.[36]

The optical signal could be amplified by the use of metal depositions after target binding events using the properties of selective and catalytic reduction of precursors on the metallic label.[37, 38] Silver is frequently used to enhance the optical signals in various ways due to its fast reduction kinetics and gray color that is visible with the naked eye.[37, 39] Gold staining has also been used to enhance the light scattering of metallic labels after the binding events,[40] and the assay showed high sensitivity (300 aM, ~9000 copies) for prostate specific antigens in buffer and 3 fM sensitivity in 10% serum.[38] In addition, signal amplification strategies using plasmonic nanoparticles are not limited in optical signal-based technology. Combining plasmonic nanoparticles with electrochemical or mechanical signal based detection methods

led to a dramatic increase in the sensitivity of each sensing scheme.[26] The gold label bound to the antibody for specific target detection could be dissolved with strong acid to produce a large number of ion species detectable using typical electrodes in the electrochemical detection system.[41] Because of the mass of nanoparticles, changes in the mechanical signals (i.e., physical deformation or resonant frequency of cantilever) have been significantly improved.[42] These results show the wide range of utility of AuNPs for improving the current limitations of biosensors.

3. Bioimaging Applications

The excellent optical properties of AuNPs have also attracted attention for bioimaging applications. The strong light scattering property due to the LSPR and robust surface chemistry enabled the use of AuNPs for sensitive imaging technologies for single cell or *in vivo* animal imaging. In this section, recently developed live cell imaging and *in vivo* imaging technologies are discussed.

3.1 Live Cell imaging

Fluorescence-based cell imaging has been the most widely used and well-established technology for life science research. However, the limited molecular information and rapid photobleaching of organic fluorophores are major issues that need to be addressed. Among various technologies, the use of plasmon nanoparticles could be an alternative technology to overcome the limitations of fluorescence-based techniques.

The strong light scattering of white light by plasmonic nanoparticles can be collected to generate images using dark-field microscopy, which is general microscopy equipped with a dark-field condenser.[43] Single spherical gold nanoparticles larger than 40 nm can be imaged as a green dot in color-CCD and a red dot when assembled into particle clusters (dimer, trimer, etc.).[24, 44] Therefore, the distribution of AuNPs in the cell can be monitored over a long period of time. El Sayed *et al*. reported changes in the optical properties of AuNPs that were associated with endocytosis of epidermal growth factor (EGF) receptors.[45] In this study, dark-field scattering images and the absorption spectra of AuNPs were compared upon binding to non-malignant and malignant cell types. Wax and Sokolov demonstrated successful imaging of actin filaments using dark-field microscopy as shown in Fig. 5a, b.[43] Obtaining sensitive dark-field cell images required the use of NIR sensitive nanoparticle structures due to the decreased autofluorescence in the NIR wavelength.[43] Therefore, NIR sensitive gold nanostructures such as AuNRs,[46] AuNSs[47] or AuCGs[48] have been actively investigated for this purpose.

Another alternative technology to fluorescence is Raman spectroscopy for imaging, as Raman scattering can provide non-bleaching molecular information for the analytes of interest. The weak signal intensity, which is a major problem in Raman spectroscopy, can be improved by generating hot spots between particles. For Raman-based cell imaging, a number of nanoparticle aggregates have been investigated to obtain high

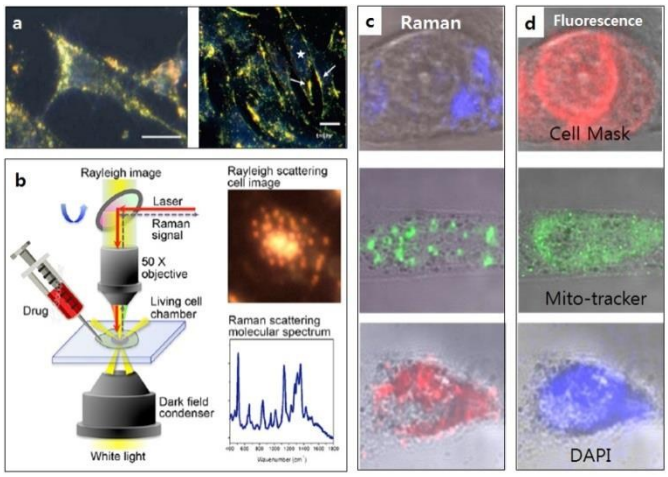

Fig. 5 (a) The dark-field images of actin filaments. (b) The experimental setup for a Rayleigh scattering image and Raman spectra. (c) High-resolution Raman images. (d) Overlapped images with fluorescence-dye. (Reprinted with permission from ref. [43, 49, 50]. Copyright 2009, WILEY-VCH Verlag, Copyright 2013, American Chemical Society, Copyright 2015, American Chemical Society).

resolution live cell Raman images and to gain information from cells.[51] However, until recently, Raman-based cell images were not comparable with fluorescence-based images because of the very low resolution and long signal acquisition time.[49] The recent advances in Raman-based cell imaging technologies demonstrate its potential for application in future bioscience. Mahajan *et al*. reported the use of intracellular SERS nanoprobes to distinguish between progenitor and differentiated cell types in a human neuroblastoma cell line.[52] SERS spectra from the nuclear region enabled identification of an increase in the DNA/RNA ratio and transcribed proteins. Furthermore, the enhanced SERS spectra by AuNPs from inside cells could be used to assess the efficacy of potential drugs based on changes in the Raman spectra and cell morphology (Fig. 5 (b)).[49] Lim *et al*. recently reported highly reproducible SERS-active nanostructures composed of a AuNP core-shell with a very narrow and uniformed intra-nanogap (ca. 1.2 nm)[53], and its use for high resolution live cell Raman images of cancer cells using a custom-built high speed confocal Raman microscope. The high resolution live cell Raman images were attained within 30 sec, and they were comparable to fluorescence-based images as shown in Fig. 5(c-d).[50]

3.2 In-vivo imaging

Plasmonic nanoparticles have been investigated as promising contrast agents for a wide range of imaging modalities such as optical imaging (i.e., NIR-based fluorescence imaging, photoacoustic imaging), computed tomography (CT),[54] and nuclear imaging (i.e., single positron emission computed tomography (SPECT) and positron emission tomography (PET)). The rapid excretion of small molecule imaging agents (i.e., iodinated contrast agents for CT) via the kidney results in short circulation times, and is therefore a major problem to be addressed in order to obtain sensitive CT imaging-based diagnoses.[55] In contrast, nano-sized imaging agents provide extended circulation in the blood stream and specific target

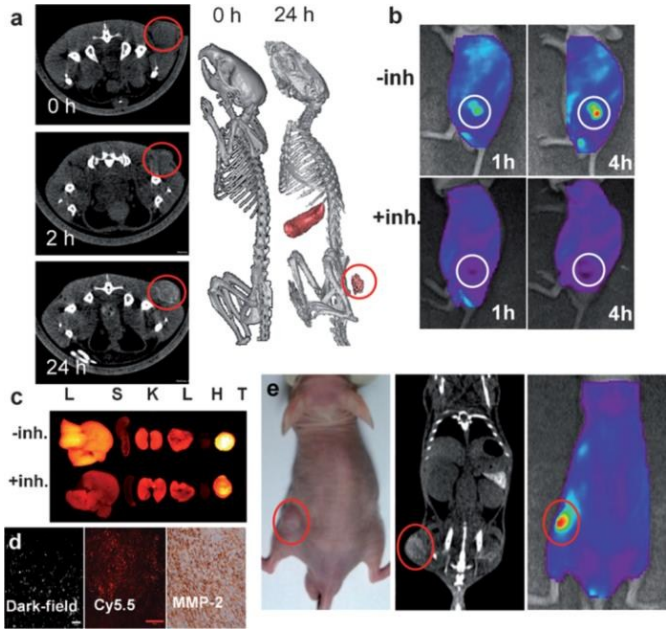

Fig. 6 (a) Cross-sectional CT images of a tumor before (0 h) and after injection (2 h, 24 h) (b) NIRF tomographic images of HT-29 tumor-bearing mice. (c) NIRF images of their organs. L: liver, S: spleen, K: kidney, L: lung, H: heart, T: tumor. (d) Dark-field (left), fluorescence (middle), and MMP-2 enzyme stained (right) microscopic images of excised HT-29 tumor tissue. Scale bar indicates 50 mm. (e) Dual CT/optical imaging of the same HT-29 tumor-bearing mouse model 24 h post-injection. (Reprinted with permission from ref. [56]. Copyright 2011, WILEY-VCH Verlag).

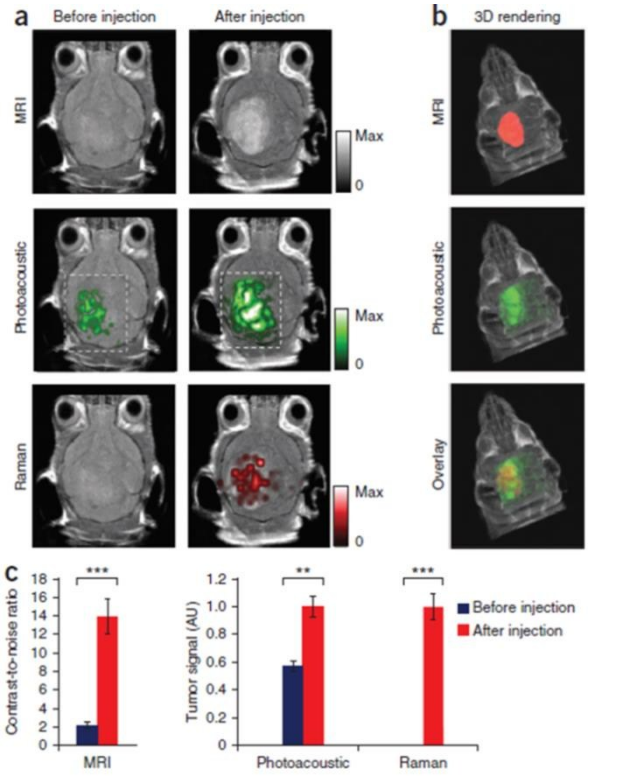

Fig. 7 Triple-modality detection of brain tumor in living mice (a) Two-dimensional axial MRI, photoacoustic and Raman images. The post-injection images of all three modalities showed clear tumor visualization (dashed boxes outline the imaged area). (b) A three-dimensional (3D) rendering of magnetic resonance images with the tumor segmented (red; top), an overlay of the three-dimensional photoacoustic images (green) over the MRI (middle) and an overlay of MRI, the segmented tumor and the photoacoustic images (bottom) showing good colocalization of the photoacoustic signal with the tumor. (c) Quantification of the signals in the tumor showing a significant increase in the MRI, photoacoustic and Raman signals after the injection that that before the injection. n = 4 mice. Data represent mean ± s.e.m. ***P < 0.001, **P < 0.01 (one-sided Student's t-test.) AU, arbitrary units. (Reprinted with permission from ref. [65]. Copyright 2012, Nature publishing group).

tissue binding properties after proper surface modifications.[55] In addition, the high atomic number (Z = 79) and k-edge value (80.7 keV) of AuNPs could induce greater contrast than iodinated contrast agents.[55] AuNPs of an average size of 1.9 nm from Nano probes Inc. were initially studied as X-ray contrast agents.[54] Although the excretion route of AuNPs is similar to that of conventional iodinated X-ray contrast agents, their clearance is slower, allowing longer imaging times. Studies to determine the optimum size and surface chemistry for efficient targeting and long circulation have been conducted by many research groups.[57] Wang *et al*. studied folic acid-modified dendrimer-entrapped AuNPs for *in vitro* and *in vivo* targeted CT imaging.[58] Ahn *et al*. reported glycol chitosan-modified AuNPs (GC-AuNPs) for tumor targeted CT imaging, and compared it to NIR fluorescence imaging activated by an abundant enzyme (matrix metalloproteinase; MMP) in the tumor (Fig. 6).[56]

AuNPs have also been investigated as nanocarriers of signaling elements for SPECT, PET, and magnetic resonance imaging (MRI) after modifying AuNPs with elements such as ^{125}I,[59] ^{124}I,[60] ^{18}F,[60] Gd,[61] ^{111}In,[62] ^{64}Cu,[63] targeting ligands and protective layers. Since each imaging modality has its own advantages and disadvantages, now researchers are focusing on the development of multimodal imaging agents. For instance, nuclear imaging (i.e., PET and SPECT) is useful for the diagnosis of diseases including cancer, but cannot provide structural information and has disadvantages such as poor spatial resolution, long scan times, non-specific uptake of radiotracers by surrounding normal tissue, and difficulty in separating signals between existing and newly formed tissue.[64] Therefore, the possible solution to overcome these limitations could be the use of multimodal imaging agents.[66] For example, Black *et al.* developed dual-radiolabeled (^{125}I and ^{111}In) AuNPs as a multispectral SPECT imaging contrast agent with an MMP cleavable peptide, and demonstrated distinct pharmacokinetic properties of the contrast agent between tumors.[62] Wang *et al*. synthesized ^{64}Cu-radiolabeled AuCGs as a dual mode (PET/CT) imaging agent, and specific AuCGs (30 nm) demonstrated a significantly improved biodistribution profile compared to AuCGs (55 nm).[67] Shi *et al*. reported dendrimer-based MRI/CT dual mode imaging agents composed of Gd(III) and small AuNPs (3.8 nm)[68-70] or Fe_3O_4 and AuNPs to exploit the benefits of each imaging modality.[68, 71] Furthermore, Kircher *et al.* reported a triple imaging modality (MRI-photoacoustic-Raman) to overcome the limitations of current imaging methods such as low sensitivity, specificity, and spatial resolution, which are strongly required to obtain clear brain tumor images. Fig.7 shows clearly distinguished MRI, photoacoustic and Raman scattering images before and after injection of the agent.[65]

The photoacoustic (PA) imaging modality provides higher resolution of acoustic images than conventional ultrasound based imaging technologies. Since the acoustic images in PA depend on the magnitudes of thermal expansions of

illuminated molecules, anisotropic gold nanostructures that can generate strong photothermal effects are excellent candidates for sensitive PA imaging agents.[48] Zharov *et al*. suggested the use of golden carbon nanotubes to obtain high PA amplitudes based on strongly enhanced PA and photothermal effects.[72] Emelianov *et al*. reported a new method for obtaining enhanced PA amplitudes by incorporating a nanoscale silica shell on gold nanorods (AuNRs), which led to decreased thermal resistance between the metallic surface and aqueous media. As a result, PA amplitudes three times higher in magnitude than naked AuNRs were attained.[73] Lim *et al*. reported reduced graphene oxide coated AuNPs as a highly efficient PA contrast agent. Experimental and mechanistic studies demonstrated that the increased light absorption and efficient heat diffusion *via* reduced graphene oxide are responsible for the five times higher PA amplitudes than naked AuNRs.[74] Ke *et al.* reported gold nanoshelled microcapsules (AuNS-MCs) for ultrasound contrast imaging, and compared to empty microcapsules, gold nanoshelled microcapsules enhanced the ultrasound imaging results.[75]

These results indicate that the unique optical properties of AuNPs could be further improved by rationally manipulating its composition or structures on the nanoscale.

4. Therapeutic Applications

The nanocarrier can alter the typical pharmacokinetics and pharmacodynamics of loaded drug molecules. Moreover, they can actively be enabled to control release kinetics using AuNPs. The recent advances in therapeutic applications based on AuNPs are discussed.

4.1 Drug delivery

For drug delivery systems, a number of amphiphilic polymers have been extensively investigated because of their safety, stability, and easy chemistry for ligand binding, as well as their high drug loading capacity. In the case of AuNPs, their inertness, high surface-to-volume ratio, and robust surface chemistry ignited their use as drug carriers. The main benefit of AuNPs for drug delivery will be use of the optical properties of AuNPs to control drug release kinetics by applying external light stimuli.[76] These capabilities are also related to the imaging and therapeutic application of AuNPs. In the earlier stages of developing AuNPs for drug delivery, researchers simply used the particles to deliver anticancer drugs loaded through physical adsorption or covalent conjugation. However, in recent studies, AuNPs are mostly used as a key component of multifunctional intelligent drug delivery systems to further improve the efficacy of anticancer drugs.

Wang *et al.* generated doxorubicin tethered AuNPs with a poly(ethylene glycol) spacer *via* an acid-labile linkage, which is a hydrazine linker, (DOX-Hyd@AuNPs) to overcome multidrug resistance in cancer cells. DOX-Hyd@AuNPs enhanced drug accumulation and retention in MCF-7/ADR cancer cells that possess multidrug resistant properties. Furthermore, DOX-

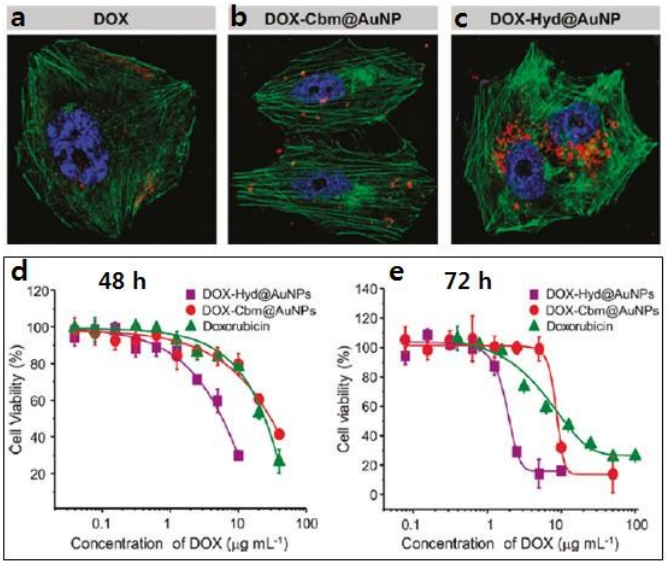

Fig. 8 Cell images after treating with (a) Doxorubicin, (b) DOX-Cbm@AuNP and (c) DOX-Hyd@AuNP. Cell viability (d) 48 h and (e) 72 h after addition of Doxorubicin, DOX-Cbm@AuNP, and DOX-Hyd@AuNP. (Reprinted with permission from ref.[77]. Copyright 2011, American Chemical Society).

Hyd@AuNPs showed highly efficient cellular entry and responsive intracellular release of doxorubicin from the AuNPs in acidic organelles, which was significantly different from that of the non acid-labile linker (DOX-Cbm@AuNPs) and free doxorubicin (Fig. 8(a-c)).[77] The DOX-Hyd@AuNPs demonstrated a stronger antitumor effect than free doxorubicin or DOX-Cbm@AuNPs as shown in Fig. 8(d-e).[77] Kumar *et al.* synthesized 2 nm size AuNPs with a therapeutic peptide, PMI (p12), and a targeted peptide (CRGDK) that binds selectively to neurophilin-1 (Nrp-1) receptors, which is overexpressed on cancer cells.[78] CRGDK functions to increase the intracellular uptake of AuNPs, and CRGDK functionalized AuNPs were maximally bound to the CRGDK peptide and the Nrp-1 receptor on the surface of MDA-MB-321 cells. This enhanced the transmission of the therapeutic P12 peptide inside target cells. Functionalized Au@p12+CRGDK nanoparticles demonstrated highly effective cancer therapy, indicating that these types of design systems composed of functionalized nanoparticles and various specific molecules onto AuNP surfaces can provide significant therapeutic effects.[78]

Xiao *et al.* developed a targeted NIR responsive nanoparticle delivery system using a simple DNA self-assembly process. *In vivo* and *in vitro* results using this NIR responsive nanoparticle system showed that drugs were selectively delivered to the target site, released by NIR irradiation, and effectively hindered cancer cell growth and progression under thermo-chemotherapy.[79] Furthermore, Song *et al.* reported the development of bioconjugated plasmonic vesicles for cancer-targeted drug delivery using self-assembled SERS-encoded amphiphilic AuNPs (Fig. 9a). The pH-sensitive hydrophobic polymer grafts in hydrophilic PEG-modified AuNPs induced sensitive disruptions in plasmonic vesicles in acidic endocytic organelles (endosome/lysosomes (pH 4.7-5.5). The SERS signal also disappeared with the disruptions in plasmonic vesicles (Fig. 9b).[80]

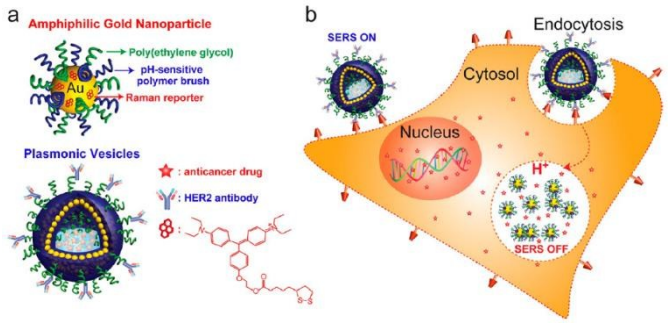

Fig. 9 (a) Schematic illustration of an amphiphilic gold nanoparticle coated with a Raman reporter and mixed polymer brushes of hydrophilic PEG and pH-sensitive hydrophobic polymer grafts, and the drug-loaded plasmonic vesicle tagged with HER2 antibody for cancer cell targeting. (b) The cellular binding, uptake, and disruption of SERS-encoded pH-sensitive plasmonic vesicles. (Reprinted with permission from ref.[80] Copyright 2012, American Chemical Society).

Thus, the use of gold nanoparticles can alter the typical pharmacokinetics of loaded drug molecules by controlling drug release and by delivering selectively loaded drugs to target cells. The combined use of AuNPs with the functionality of polymers or chemical linkers could be smart tools to greatly improve the therapeutic efficacy of conventional drugs of interest.

4.2 Photothermal therapy (PTT)

The ability of AuNPs to efficiently absorb visible and NIR light depends on the structures, and the absorbed energy converted into local heat energy through the fast non-radioactive decay process.[13] The local heat induces significant damage to abnormal cells. Specifically, cancerous cells are more susceptible to the heat damage than normal cells, demonstrating that efficient cell death can be initiated in tumor cells containing AuNPs.[13] Since use of the NIR region of light can maximize the penetration depth of light into body-tissues, anisotropic gold nanostructures such as gold nanorods (AuNRs),[81] nanoshells (AuNSs),[82] nanocages (AuCGs)[83] and nanostars (AuSTs)[13, 84] that have LSPR absorption at 700 – 900 nm are frequently used for efficient photothermal therapy.[13]

A number of strategies for generating efficient photothermal effects have been investigated. Developing strategies to increase the uptake efficiency of nanoparticles into target cells can significantly reduce the concentration of nanoparticles as well as the light dose. To achieve these goals, a wide range of strategies have been employed. Wang *et al.* presented target specific AuNRs to efficiently destroy tumor cells by allowing their accumulation in the mitochondria, which is a critical subcellular organelle that maintains the homeostasis of cells.[85] Yuan *et al*. generated TAT peptide-functionalized gold nanostars (TAT-AuSTs) to remarkably improve intracellular uptake efficiency and induce a strong photothermal effect.[15] The TAP-peptide is a cell penetrating peptide (CPP), obtained from human immunodeficiency virus type 1, that can facilitate particle uptake. The gold nanostars generated strong photothermal effects in response to 850 nm laser excitation.[15] Similarly, branched gold nanoparticles functionalized with anti-HER2 antibody to treat breast cancer demonstrated specific cell targeting and effective photothermal effect.[86]

Developing new materials that can absorb NIR-light efficiently is another promising method for achieving an improved photothermal effect. In this regard, new nanocomposites composed of gold and additional efficient visible-NIR light absorbing materials such as silicon nanowire,[87] carbon nanotube,[88] or reduced graphene oxide[89] have been investigated. Lim *et al*. recently reported reduced graphene oxide coated gold nanorods or gold nanoshells for enhanced photothermal effects. Interestingly, only reduced graphene oxide coated NPs showed significantly increased photothermal effect due to the recovered electronic state of reduced graphene oxide.[89] The application of enhanced photothermal properties can be extended to other areas such as improved photoacoustic applications,[74] live cell imaging,[88] or NIR-responsive intelligent drug delivery systems.

The important limiting factor of photothermal therapy using AuNPs is the penetration depth of light energy through body tissues. In contrast, the magnetic field and radio-frequency (RF) field have no such depth limitation, therefore biocompatible materials that can sensitively respond to RF would be promising candidates for future hyperthermia-based therapeutic applications.[90] In this regard, controversy over the magnetism of AuNPs is quite interesting.[91] Recently, McCoy *et al*. reported that the $Au_{102}(pMBA)_{44}$ nanocluster becomes paramagnetic when oxidized with $KMnO_4$, such that they can be heated by magnetic fields, similar to the heating of magnetic NPs (such as iron oxide NPs) in oscillating magnetic fields. In this type of heating, particles can rotate within the stationary solvent (Brownian relaxation) or magnetic dipoles can rotate within the particle (Neel relaxation).[91,92] These results present a new potential of AuNPs for RF and resulting hyperthermia-based therapeutic applications.

Because of the discussed optical and physical properties, AuNPs also play a central role in theranostic applications. The photothermal effects of AuNPs, in addition to their direct therapeutic application, are also used to trigger drug delivery to target tissues with the capability to simultaneously monitor the disease state.[93-95] AuNRs,[96] AuNSs,[75, 82] AuCGs[97] and AuSTs[98] have frequently been used for this purpose. Shi *et al.* recently demonstrated the utility of a combination of Fe_3O_4 and AuSTs for dual mode imaging (MRI/CT) and the strong photothermal effects of AuSTs.[71]

5. Tissue Engineering Applications

For tissue engineering applications, active tools that can control the behavior or fate of cells to properly generate target tissues are strongly required. Biocompatible polymers with or without bioconjugation have been widely investigated for this purpose. With increased understanding of the interaction between nanomaterials and biomolecules,[99] a wide range of nanomaterials have been employed for tissue engineering applications. The interactions of cells on substrates are quite

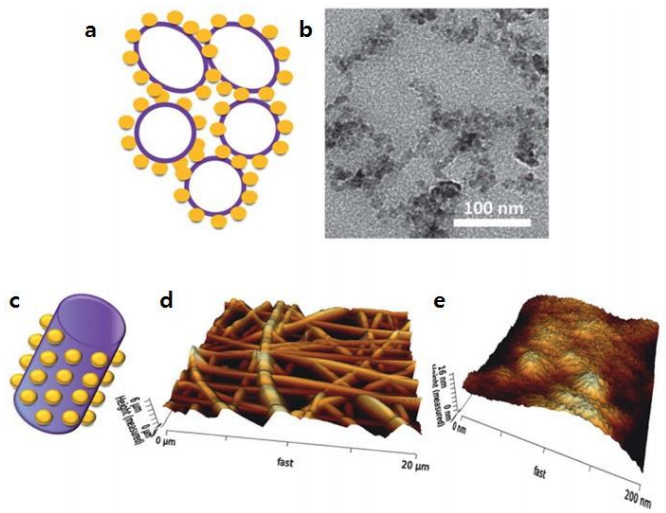

Fig. 10 AuNPs on the fibers. (a) Illustration of a fiber cross-section. (b) Cross-sectional transmission electron microscopy (TEM) of the fibers coated with gold NPs. Bar = 100 nm. (c) Illustration of a single fiber covered with gold NPs. (d) Topography of gold NP fibers by atomic force microscopy (AFM). (e) Topography of gold NPs (4 nm) on a single fiber. (Reprinted with permission from ref.[100] Copyright 2013, Royal Chemical Society).

complex. A number of parameters such as nanostructures, stiffness, hardness, and surface functionality and properties significantly influence the fate of cells. For this reason, AuNPs have been investigated as biocompatible materials that can easily generate nano-featured 2D and 3D structures with excellent physical properties (Fig. 10). Mukhopadhyay *et al*. highlighted the biological function of AuNPs by demonstrating their potential to induce an antiangiogenic effect. They showed that AuNPs could inhibit the angiogenic factor $VEGF_{165}$.[101] Binding of AuNPs to the heparin binding domain of VEGF was possibly the reason for the observed inhibitory effect, which ignited a series of related studies.[101-103] Detailed investigations on the controllable parameters of AuNPs with specific cell types have been extensively performed.[104]

Recently, Heo *et al*. reported the use of curcumin conjugated AuNPs as a therapeutic agent for preventing and treating osteoporosis. It has been known that AuNPs inhibit osteoclast formation but the osteoclastogenic inhibitory effect was possible only *in vitro* conditions. In this study, the osteoclastogenic inhibitory effect was demonstrated using curcumin conjugated AuNPs *in vivo*.[105] Shevach *et al*., through immunocytochemistry, demonstrated that AuNPs of various sizes with polycaprolactone-gelatin fiber can trigger the elongation and alignment of cardiac cells on composites.[106] Hung *et al.* studied the effect of gold nanoparticles in collagen composites on the behavior of mesenchymal stem cells (MSCs).[107] Fabrication of a biomimicking environment for growing MSCs is an area that needs further investigation, because the adhesion/proliferation capacity of vascular endothelial cells and MSCs for vascular grafts is generally poor. This study demonstrated that a specific concentration of AuNPs (43.5 ppm) promotes adhesion, proliferation, and migration of MSCs. Furthermore, the AuNPs induced a reduced inflammatory response and served as a regulator of the αvβ3 integrin/CXCR4 receptor, FAK, MMP-2, and Akt/eNOS molecular signaling pathways for the promotion of stem cell differentiation to vascular endothelial cells, which is mediated by VEGF/SDF-1α.[107] Yi *et al*. also studied the interactions between AuNPs and cells and these relationships promoted osteogenic differentiation of MSCs through the p38 MAPK pathway. The interaction of AuNPs with the extracellular matrix was induced via the up-regulation of integrin, which caused cellular stress on the MSCs, leading to activation of the p38 MAPK pathway.[109]

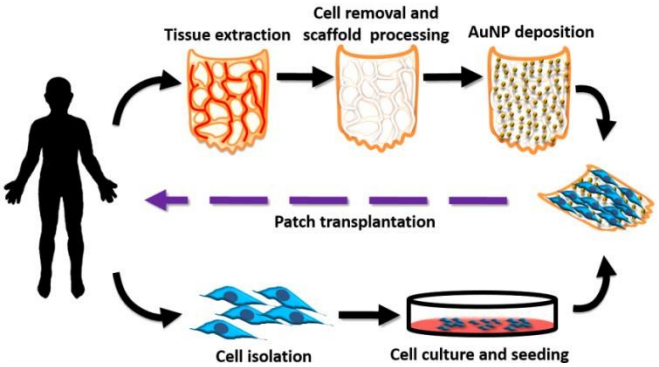

Fig. 11 Schematic overview of cardiac tissue engineering. Isolation of omental tissue from the patient, a quick decellularization process, and AuNP deposition. Isolation of cells from the same patient, cultured in vitro, and seeded on the hybrid scaffold to produce a personalized cardiac patch and subsequent patch transplantation. (Reprinted with permission from ref. [108] Copyright 2014, American Chemical Society).

For efficient cardiac cell engineering, gold nanowires can be used to control cardiac cells more efficiently. Engineered cardiac patches for treating damaged heart tissues after a heart attack are normally produced by seeding heart cells in three-dimensional porous biomaterial scaffolds. Incorporating gold nanowires within biocompatible polymer scaffolds (i.e., alginate) can bridge the electrically resistant pore walls of alginate and improve electrical communication between adjacent cardiac cells.[104] D. Tal *et al.* explored the potential of AuNPs to improve the structural and functional assembly of cardiac tissues grown within coiled fiber scaffolds to overcome the limited ability of the scaffolds to propagate the electrical signals between cultured cardiac cells by evaporating AuNPs with a nominal thickness of 10 nm onto the surface of the fiber.[100] The AuNP-decellularized matrix hybrid can affect the function of cardiac tissue engineering, and the electrical signal is 2- to 3-fold faster than in omental matrices (Fig. 11).[108] This indicates that a hybrid patch with AuNPs can improve the efficacy of cardiac therapy *in vivo*. As a surface modifier and an agent for releasing factors, AuNPs can be applied to the fabrication of scaffolds. Additionally, they can promote cell behavior and regulate cell signaling. Thus, these results suggest that gold-based materials can be useful scaffolds for engineering various tissues along with providing effective additional functions.

6. Conclusions

Here, we reviewed recent advances in biomedical engineering applications based on the unique and useful properties of AuNPs. The applications include biosensing schemes for

sensitive nucleic acid and protein detection, *in vitro* and *in vivo* bioimaging, therapeutic applications for intelligent drug delivery systems, photothermal effect-based therapy, and tissue engineering. In most bioengineering applications, AuNPs have played a key role in generating breakthrough technology due to its diverse and controllable functionality. As evidenced by the successful commercialization of gold based technologies such as Verigene® and Biacore® as new tools for bioscience, new breakthrough technologies in the field of therapeutics are also expected in the near future.

However, two key issues still remain unsolved, and need to be addressed for future clinical applications of AuNPs. The primary issue is the potential toxicity of AuNPs, which requires careful investigation. Another intrinsic limitation for bioengineering applications is the limited penetration depth of visible-NIR light into body tissues, which is the same problem observed in fluorescence-based optical imaging technology. New materials that can strongly absorb external light energy or internal energy (i.e., chemiluminescence) will be a possible solution. Furthermore, developing new optics that can overcome the current limitations of penetration depth is another promising solution.[110] In this regard, it is expected that there will be another golden age of AuNPs for future basic science, including chemistry, physics, biology, biochemistry, and bioengineering for the development of biosensors, bioimaging, and nanomedicine.

Acknowledgements

This work was supported by the National Research Foundation of Korea (NRF-2013R1A1A1061387) and the KU-KIST research fund.

Notes and references

1. A. S. Thakor, J. Jokerst, C. Zavaleta, T. F. Massoud and S. S. Gambhir, *Nano Lett.*, 2011, **11**, 4029-4036.
2. I. Ujfalussy, E. Koo, M. Sesztak and P. Gergely, *Z. Rheumatol.*, 2003, **62**, 155.
3. G. D. Champion, G. G. Graham and J. B. Ziegler, *Baillieres Clin. Rheumatol.*, 1990, **4**, 491.
4. K. Dalziel, G. Going, P. H. Cartwright, R. Marks, G. W. Beveridge and N. R. Rowell, *Br. J. Dermatol.*, 1986, **115**, 211.
5. E. C. Dreaden, A. M. Alkilany, X. Huang, C. J. Murphy and M. A. El-Sayed, *Chem. Soc. Rev.*, 2012, **41**, 2740-2779.
6. J. M. Bingham, K. A. Willets, N. C. Shah, D. Q. Andrews and R. P. Van Duyne, *J. Phys. Chem. C*, 2009, **113**, 16839-16842.
7. S. Link and M. A. El-Sayed, *J. Phys. Chem. B*, 1999, **103**, 4212-4217.
8. N. J. Halas, *Nano Lett.*, 2010, **10**, 3816-3822.
9. H. A. Atwater and A. Polman, *Nat. Mater.*, 2010, **9**, 205-213.
10. D. P. Yang and D. X. Cui, *Chem.—Asian J.*, 2008, **3**, 2010.
11. P. AshaRani, G. Low Kah Mun, M. P. Hande and S. Valiyaveettil, *ACS Nano*, 2008, **3**, 279-290.
12. J. Kimling, M. Maier, B. Okenve, V. Kotaidis, H. Ballot and A. Plech, *J. Phys. Chem. B*, 2006, **110**, 15700.
13. Y. Wang, K. C. Black, H. Luehmann, W. Li, Y. Zhang, X. Cai, D. Wan, S.-Y. Liu, M. Li and P. Kim, *ACS Nano*, 2013, **7**, 2068-2077.
14. S. Lal, S. L. Westcott, R. N. Taylor, J. B. Jackson, P. Nordlander and N. J. Halas, *J. Phys. Chem. B*, 2002, **106**, 5609-5612.
15. H. Yuan, A. M. Fales and T. Vo-Dinh, *J. Am. Chem. Soc.*, 2012, **134**, 11358-11361.
16. M. A. Mackey, M. R. K. Ali, L. A. Austin, R. D. Near and M. A. El-Sayed, *J. Phys. Chem. B*, 2014, **118**, 1319-1326.
17. A. M. Funston, C. Novo, T. J. Davis and P. Mulvaney, *Nano Lett.*, 2009, **9**, 1651-1658.
18. S. Lin, E. Dujardin, C. Girard and S. Mann, *Adv. Mater.*, 2005, **17**, 2553-2559.
19. K. H. Su, Q. H. Wei and X. Zhang, *Nano Lett.*, 2003, **3**, 1087-1090.
20. C. A. Mirkin, R. L. Letsinger, R. C. Mucic and J. J. Storhoff, *Nature*, 1996, **382**, 607-609.
21. A. P. Alivastos, *Nature*, 1996, **382**, 609-611.
22. J. J. Storhoff, R. Elghanian, R. C. Mucic, C. A. Mirkin and R. L. Letsinger, *J. Am. Chem. Soc.*, 1998, **120**, 1959-1964.
23. N. Liu, M. Hentschel, T. Weiss, A. P. Alivisatos and H. Giessen, *Science*, 2011, **332**, 1407-1410.
24. C. Sonnichsen, B. M. Reinhard, J. Liphardt and A. P. Alivisatos, *Nat. Biotechnol.*, 2005, **6**, 741-745.
25. G. Qiao, Y. Gao, N. Li, Z. Yu, L. Zhuo and B. Tang, *Chem. Eur. J.*, 2011, **17**, 11210-11215.
26. J. Jeon, D.-K. Lim and J.-M. Nam, *J. Mater. Chem.* 2009, **19**, 2107-2117.
27. J. J. Storhoff, A. D. Lucas, V. Garimella, Y. P. Bao and U. R. Muller, *Nat. Biotechnol.*, 2004, **22**, 883-887.
28. M. Cottat, N. Thioune, A.-M. Gabudean, N. Lidgi-Guigui, M. Focsan, S. Astilean and M. Lamy de la Chapelle, *Plasmonics*, 2013, **8**, 699-704.
29. W. P. Hall, S. N. Ngatia and R. P. Van Duyne, *J. Phys. Chem. C*, 2011, **115**, 1410-1414.
30. C. D. Medley, J. E. Smith, Z. Tang, Y. Wu, S. Bamrungsap and W. Tan, *Anal. Chem.,* 2008, **80**, 1067-1072.
31. A. Abbas, L. Tian, J. J. Morrissey, E. D. Kharasch and S. Singamaneni, *Adv. Funct. Mater.* 2013, **23**, 1789-1797.
32. S. Zeng, D. Baillargeat, H.-P. Ho and K.-T. Yong, *Chem. Soc. Rev.,* 2014, **43**, 3426-3452.
33. O. Salihoglu, S. Balci and C. Kocabas, *Appl. Phys. Lett.,* 2012, **100**, 213110.
34. H. Im, H. Shao, Y. I. Park, V. M. Peterson, C. M. Castro, R. Weissleder and H. Lee, *Nat. Biotechnol.*, 2014, **32**, 490-495.
35. Y. C. Cao, R. Jin and C. A. Mirkin, *Science*, 2002, **297**, 1536-1540.
36. E. C. Le Ru, M. Meyer and P. G. Etchegoin, *J. Phys. Chem. B*, 2006, **110**, 1944-1948.
37. T. A. Taton, C. A. Mirkin and R. L. Letsinger, *Science*, 2000, **289**, 1757-1760.
38. D. Kim, W. L. Daniel and C. A. Mirkin, *Anal. Chem.*, 2009, **81**, 9183-9187.
39. S.-Y. Shim, J.-R. Woo, E.-J. Nam, H.-J. Hong, I. Mook-Jung, Y.-H. Kim and J.-M. Nam, *Nanomedicine,* 2008, **3**, 485-493.
40. Z. Ma and S.-F. Sui, *Angew. Chem. Int. Edit*, 2002, **41**, 2176-2179.
41. Z. Zhu, Y. Su, J. Li, D. Li, J. Zhang, S. Song, Y. Zhao, G. Li and C. Fan, *Anal. Chem.*, 2009, **81**, 7660-7666.

42. M. Su, S. Li and V. P. Dravid, *Appl. Phy. Lett.*, 2003, **82**, 3562-3564.
43. A. Wax and K. Sokolov, *Laser Photon Rev.*, 2009, **3**, 146-158.
44. C. L. Choi and A. P. Alivisatos, *Annu. Rev. Phys. Chem.*, 2010, **61**, 369-389.
45. I. H. El-Sayed, X. Huang and M. A. El-Sayed, *Nano Lett.*, 2005, **5**, 829-834.
46. K. C. Black, N. D. Kirkpatrick, T. S. Troutman, L. Xu, J. Vagner, R. J. Gillies, J. K. Barton, U. Utzinger and M. Romanowski, *Mol. Imaging*, 2008, **7**, 50.
47. C. Loo, A. Lowery, N. Halas, J. West and R. Drezek, *Nano Lett.*, 2005, **5**, 709-711.
48. C. Kim, E. C. Cho, J. Chen, K. H. Song, L. Au, C. Favazza, Q. Zhang, C. M. Cobley, F. Gao and Y. Xia, *ACS Nano*, 2010, **4**, 4559-4564.
49. L. A. Austin, B. Kang and M. A. El-Sayed, *J. Am. Chem. Soc.*, 2013, **135**, 4688-4691.
50. J. W. Kang, P. T. C. So, R. R. Dasari and D.-K. Lim, *Nano Lett.*, 2015, **15**, 1766-1772.
51. J. Kneipp, H. Kneipp, M. McLaughlin, D. Brown and K. Kneipp, *Nano Lett.*, 2006, **6**, 2225-2231.
52. A. Huefner, W.-L. Kuan, R. A. Barker and S. Mahajan, *Nano Lett.*, 2013, **13**, 2463-2470.
53. D.-K. Lim, K.-S. Jeon, J.-H. Hwang, H. Kim, S. Kwon, Y. D. Suh and J.-M. Nam, *Nat. Nanotechnol.*, 2011, **6**, 452-460.
54. J. F. Hainfeld, D. N. Slatkin, T. M. Focella and H. M. Smilowitz, *Brit. J. Radiol.*, 2006, **79**, 248-253.
55. N. Lee, S. H. Choi and T. Hyeon, *Adv. Mater.*, 2013, **25**, 2641-2660.
56. I. C. Sun, D. K. Eun, H. Koo, C. Y. Ko, H. S. Kim, D. K. Yi, K. Choi, I. C. Kwon, K. Kim and C. H. Ahn, *Angew. Chem. Int. Edit*, 2011, **123**, 9520-9523.
57. J. Liu, M. Yu, X. Ning, C. Zhou, S. Yang and J. Zheng, *Angew. Chem. Int. Edit*, 2013, **125**, 12804-12808.
58. H. Wang, L. Zheng, C. Peng, M. Shen, X. Shi and G. Zhang, *Biomaterials*, 2013, **34**, 470-480.
59. Y. H. Kim, J. Jeon, S. H. Hong, W. K. Rhim, Y. S. Lee, H. Youn, J. K. Chung, M. C. Lee, D. S. Lee and K. W. Kang, *Small*, 2011, **7**, 2052-2060.
60. D. P. Cormode, E. Roessl, A. Thran, T. Skajaa, R. E. Gordon, J.-P. Schlomka, V. Fuster, E. A. Fisher, W. J. Mulder and R. Proksa, *Radiology*, 2010.
61. L. Moriggi, C. Cannizzo, E. Dumas, C. R. Mayer, A. Ulianov and L. Helm, *J. Am. Chem. Soc.*, 2009, **131**, 10828-10829.
62. K. C. Black, W. J. Akers, G. Sudlow, B. Xu, R. Laforest and S. Achilefu, *Nanoscale*, 2015, **7**, 440-444.
63. Y. Zhao, D. Sultan, L. Detering, S. Cho, G. Sun, R. Pierce, K. L. Wooley and Y. Liu, *Angew. Chem. Int. Edit*, 2014, **53**, 156-159.
64. J. Key and J. F. Leary, *Int. J. Nanomedicine*, 2014, **9**, 711.
65. M. F. Kircher, A. de la Zerda, J. V. Jokerst, C. L. Zavaleta, P. J. Kempen, E. Mittra, K. Pitter, R. Huang, C. Campos, F. Habte, R. Sinclair, C. W. Brennan, I. K. Mellinghoff, E. C. Holland and S. S. Gambhir, *Nat. Med.*, 2012, **18**, 829-834.
66. J. Zhang, C. Li, X. Zhang, S. Huo, S. Jin, F.-F. An, X. Wang, X. Xue, C. Okeke and G. Duan, *Biomaterials*, 2015, **42**, 103-111.
67. Y. Wang, Y. Liu, H. Luehmann, X. Xia, P. Brown, C. Jarreau, M. Welch and Y. Xia, *ACS Nano*, 2012, **6**, 5880-5888.
68. Q. Chen, H. Wang, H. Liu, S. Wen, C. Peng, M. Shen, G. Zhang and X. Shi, *Anal. Chem.*, 2015, **87**, 3949-3956.
69. Q. Chen, K. Li, S. Wen, H. Liu, C. Peng, H. Cai, M. Shen, G. Zhang and X. Shi, *Biomaterials*, 2013, **34**, 5200-5209.
70. S. Wen, K. Li, H. Cai, Q. Chen, M. Shen, Y. Huang, C. Peng, W. Hou, M. Zhu, G. Zhang and X. Shi, *Biomaterials*, 2013, **34**, 1570-1580.
71. J. Li, Y. Hu, J. Yang, P. Wei, W. Sun, M. Shen, G. Zhang and X. Shi, *Biomaterials*, 2015, **38**, 10-21.
72. J.-W. Kim, E. I. Galanzha, E. V. Shashkov, H.-M. Moon and V. P. Zharov, *Nat. Nanotechnol.,* 2009, **4**, 688-694.
73. Y.-S. Chen, W. Frey, S. Kim, P. Kruizinga, K. Homan and S. Emelianov, *Nano Lett.*, 2011, **11**, 348-354.
74. H. Moon, D. Kumar, H. Kim, C. Sim, J.-H. Chang, J.-M. Kim, H. Kim and D.-K. Lim, *ACS Nano*, 2015, **9**, 2711-2719.
75. H. Ke, J. Wang, Z. Dai, Y. Jin, E. Qu, Z. Xing, C. Guo, X. Yue and J. Liu, *Angew. Chem. Int. Edit*, 2011, **50**, 3017-3021.
76. M. S. Khan, G. D. Vishakante and H. Siddaramaiah, *Adv. Colloid Interface Sci.*, 2013, **199-200**, 44-58.
77. F. Wang, Y.-C. Wang, S. Dou, M.-H. Xiong, T.-M. Sun and J. Wang, *ACS Nano*, 2011, **5**, 3679-3692.
78. A. Kumar, H. Ma, X. Zhang, K. Huang, S. Jin, J. Liu, T. Wei, W. Cao, G. Zou and X. J. Liang, *Biomaterials*, 2012, **33**, 1180-1189.
79. Z. Xiao, C. Ji, J. Shi, E. M. Pridgen, J. Frieder, J. Wu and O. C. Farokhzad, *Angew. Chem. Int. Ed. Engl*, 2012, **51**, 11853-11857.
80. J. Song, J. Zhou and H. Duan, *J. Am. Chem. Soc.*, 2012, **134**, 13458-13469.
81. A. M. Alkilany, L. B. Thompson, S. P. Boulos, P. N. Sisco and C. J. Murphy, *Adv. Drug Deliv. Rev.*, 2012, **64**, 190-199.
82. S. Lal, S. E. Clare and N. J. Halas, *Acc. Chem. Rev.*, 2008, **41**, 1842-1851.
83. J. Chen, B. Wiley, W.Y. Li, D. Campbell, F. Saeki, H. Cang, L. Au, J. Lee, X. Li and Y. Xia, *Adv. Mater.*, 2005, **17**, 2255-2261.
84. J. Li, R. Cai, N. Kawazoe and G. Chen, *J. Mater. Chem. B*, 2015, **3**, 5806-5814
85. L. Wang, Y. Liu, W. Li, X. Jiang, Y. Ji, X. Wu, L. Xu, Y. Qiu, K. Zhao, T. Wei, Y. Li, Y. Zhao and C. Chen, *Nano Lett.*, 2011, **11**, 772-780.
86. B. V. Broek, N. Devoogdt, A. D'Hollander, K. J. Hannah-Laura Gijs, L. Lagae, S. Muyldermans, G. Maes and G. Borghs, *ACS Nano*, 2011, **5**, 4319-4328.
87. Y. Su, X. Wei, F. Peng, Y. Zhong, Y. Lu, S. Su, T. Xu, S.-T. Lee and Y. He, *Nano Lett.*, 2012, **12**, 1845-1850.
88. X. Wang, C. Wang, L. Cheng, S.-T. Lee and Z. Liu, *J. Am. Chem. Soc.*, 2012, **134**, 7414-7422.
89. D.-K. Lim, A. Barhoumi, R. G. Wylie, G. Reznor, R. S. Langer and D. S. Kohane, *Nano Lett.*, 2013, **13**, 4075-4079.
90. K. P. Tamarov, L. A. Osminkina, S. V. Zinovyev, K. A. Maximova, J. V. Kargina, M. B. Gongalsky, Y. Ryabchikov, A. Al-Kattan, A. P. Sviridov and M. Sentis, *Sci. Rep.*, 2014, **4**. 7034
91. H.K. Kim, G.W. Hanson and D. A Geller, Science, 2013, **340** (6131), 441-442.
92. R. S. McCoy, S. Choi, G. Collins, B. J. Ackerson and C. J. Ackerson, *ACS Nano*, 2013, **7**, 2610-2616.
93. X. Yang, X. Liu, Z. Liu, F. Pu, J. Ren and X. Qu, *Adv. Mater.*, 2012, **24**, 2890-2895.
94. J. You, G. Zhang and C. Li, *ACS Nano*, 2010, **4**, 1033-1041.
95. A. M. Alkilany, L. B. Thompson, S. P. Boulos, P. N. Sisco and C. J. Murphy, *Adv. Drug Deliv. Rev.*, 2012, **64**, 190-199.

96. Z. Zhang, L. Wang, J. Wang, X. Jiang, X. Li, Z. Hu, Y. Ji, X. Wu and C. Chen, *Adv. Mater.*, 2012, **24**, 1418-1423.
97. Y. Xia, W. Li, C. M. Cobley, J. Chen, X. Xia, Q. Zhang, M. Yang, E. C. Cho and P. K. Brown, *Acc. Chem. Res.*, 2011, **44**, 914-924.
98. A. M. Fales, H. Yuan and T. Vo-Dinh, *Langmuir*, 2011, **27**, 12186-12190.
99. Q. Mu, G. Jiang, L. Chen, H. Zhou, D. Fourches, A. Tropsha and B. Yan, *Chem. Rev.*, 2014, **114**, 7740-7781.
100. M. Shevach, B. M. Maoz, R. Feiner, A. Shapira and T. Dvir, *J. Mater. Chem. B*, 2013, **1**, 5210.
101. R. Bhattacharya, P. Mukherjee, Z. Xiong, A. Atala, S. Soker and D. Mukhopadhyay, *Nano Lett.*, 2004, **4**, 2479-2481.
102. D. Bartczak, O. L. Muskens, T. Sanchez-Elsner, A. G. Kanaras and T. M. Millar, *ACS Nano*, 2013, **7**, 5628-5636.
103. H. Lee, M.-Y. Lee, S. H. Bhang, B.-S. Kim, Y. S. Kim, J. H. Ju, K. S. Kim and S. K. Hahn, *ACS Nano*, 2014, **8**, 4790-4798.
104. T. Dvir, B. P. Timko, D. S. Kohane and R. Langer, *Nat. Nanotechnol.,* 2011, **6**, 13-22.
105. D. N. Heo, W.-K. Ko, H.-J. Moon, H.-J. Kim, S. J. Lee, J. B. Lee, M. S. Bae, J.-K. Yi, Y.-S. Hwang, J. B. Bang, E.-C. Kim, S. H. Do and I. K. Kwon, *ACS Nano*, 2014, **8**, 12049-12062.
106. M. Shevach, B. M. Maoz, R. Feiner, A. Shapira and T. Dvir, *J. Mater. Chem. B*, 2013, **1**, 5210-5217.
107. H.-S. Hung, C.-H. Chang, C.-J. Chang, C.-M. Tang, W.-C. Kao, S.-Z. Lin, H.-H. Hsieh, M.-Y. Chu, W.-S. Sun and S.-h. Hsu, 2014, PLoS ONE 9(8): e104019.
108. M. Shevach, S. Fleischer, A. Shapira and T. Dvir, *Nano Lett*, 2014, **14**, 5792-5796.
109. C. Yi, D. Liu, C.-C. Fong, J. Zhang and M. Yang, *ACS Nano*, 2010, **4**, 6439-6448.
110. M. Kim, Y. Choi, C. Yoon, W. Choi, J. Kim, Q.-H. Park and W. Choi, *Nat. Photonics*, 2012, **6**, 581-585.

Table of Contents

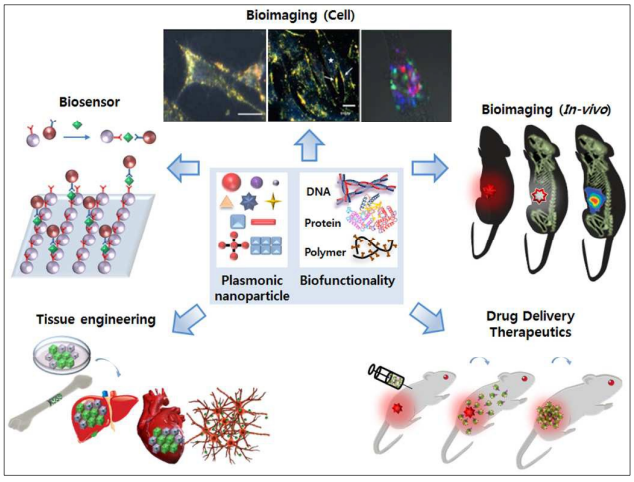

The recently developed gold nanoparticle-based bioengineering technologies for biosensors, *in vitro* and *in vivo* bioimaging, drug delivery systems for improved therapeutics and tissue engineering are discussed.